Neural Networks 98 (2018) 271–282

Contents lists available at ScienceDirect

Neural Networks

journal homepage: www.elsevier.com/locate/neunet

Modeling spike-wave discharges by a complex network of neuronal oscillators

Tatiana M. Medvedeva [a,b,*], Marina V. Sysoeva [c], Gilles van Luijtelaar [d], Ilya V. Sysoev [a,e]

[a] Saratov State University, 410012, Saratov, 83, Astrakhanskaya str., Russia
[b] Institute of Higher Nervous Activity and Neurophysiology RAS, 5A, Butlerova str., Moscow, Russia
[c] Yuri Gagarin State Technical University of Saratov, Saratov, Russia
[d] Donders Centre for Cognition, Radboud University, Nijmegen, The Netherlands
[e] Saratov Branch of V. A. Kotelnikov Institute of Radio-engineering and Electronics of the Russian Academy of Sciences, 38 Zelyonaya St., Saratov 410019, Russia

HIGHLIGHTS

- Hierarchically organized networks of neuronal oscillators generate SWDs.
- Main characteristics (amplitude rise, main frequency, harmonics) were simulated.
- Stability of model to variation of structure and scaling was shown.
- Results of coupling analysis from experimental data were reproduced by the model.
- Specific pathological changes in brain architecture might be needed for SWDs.

ARTICLE INFO

Article history:
Received 26 April 2017
Received in revised form 2 October 2017
Accepted 4 December 2017
Available online 13 December 2017

Keywords:
Spike-wave discharges
Complex networks
Absence epilepsy
Mathematical modeling
Genetic absence models
Granger causality

ABSTRACT

Purpose: The organization of neural networks and the mechanisms, which generate the highly stereotypical for absence epilepsy spike-wave discharges (SWDs) is heavily debated. Here we describe such a model which can both reproduce the characteristics of SWDs and dynamics of coupling between brain regions, relying mainly on properties of hierarchically organized networks of a large number of neuronal oscillators.

Model: We used a two level mesoscale model. The first level consists of three structures: the nervus trigeminus serving as an input, the thalamus and the somatosensory cortex; the second level of a group of nearby situated neurons belonging to one of three modeled structures.

Results: The model reproduces the main features of the transition from normal to epileptiformic activity and its spontaneous abortion: an increase in the oscillation amplitude, the emergence of the main frequency and its higher harmonics, and the ability to generate trains of seizures. The model was stable with respect to variations in the structure of couplings and to scaling. The analyzes of the interactions between model structures from their time series using Granger causality method showed that the model reproduced the preictal coupling increase detected previously from experimental data.

Conclusion: SWDs can be generated by changes in network organization. It is proposed that a specific pathological architecture of couplings in the brain is necessary to allow the transition from normal to epileptiformic activity, next to by others modeled and reported factors referring to complex, intrinsic, and synaptic mechanisms.

1. Introduction

Absence epilepsy is a generalized form of epilepsy which is characterized by a transient diminishment of the level of consciousness and responsiveness with only minimal, mainly facial movements. This form of epilepsy is mainly present in children and adolescents (Panayiotopoulos, 2001), and it may either remit (Berg, Levy, Testa, & Blumenfeld, 2014) or transform into

* Corresponding author at: Saratov State University, 410012, Saratov, 83, Astrakhanskaya str., Russia.

E-mail addresses: golovatanya@rambler.ru (T.M. Medvedeva), bobrichek@mail.ru (M.V. Sysoeva), g.vanluijtelaar@donders.ru.nl (G. van Luijtelaar), ivssci@gmail.com (I.V. Sysoev).

https://doi.org/10.1016/j.neunet.2017.12.002
0893-6080/

other, convulsive forms with time (Sadleir, Farrell, Smith, et al., 2006). The study of the pathophysiology of absence epilepsy has revealed a variety of potential mechanisms of absence seizures occurrence (Crunelli & Leresche, 2002; Depaulis & Charpier, 2017; van Luijtelaar, Hramov, Sitnikova, & Koronovskii, 2011).

Electroencephalography is the main method to register manifestations of absence epilepsy, since EEG recordings show the typical spike-wave discharges (SWDs) during absence seizures. Traditional scalp EEGs are commonly used for diagnosis, however subcortical structures (primary different nuclei of thalamus) are considered to play a significant role in absence seizure spreading and maintenance, as was established in the genetic rodent models (Depaulis & Charpier, 2017; Inoue, Duysens, Vossen, & Coenen, 1993; Sitnikova & van Luijtelaar, 2007), in a single patient with depth electrodes (Williams, 1953), and more recently with fMRI, both in the genetic animal models (Tenney, Duong, King, & Ferris, 200) and in patients (Moeller et al., 2010). Patients suffering from absence epilepsy have no clinical indication for implantation of intracranial electrodes considering that the disease is relatively benign, therefore the main results regarding the role of the thalamus were obtained using genetic rat models such as WAG/Rij (Coenen & van Luijtelaar, 2003) and GAERS (Marescaux, Vergnes, & Depaulis, 1992).

In order to understand the mechanisms of absence epilepsy, it is important to build a mathematical model (here and further we use term "model" in sense of a mathematical model, not a biological, genetic or pharmacological one, except when it is explicitly mentioned) reproducing some of the main features: sudden onset and termination of SWDs, chemical processes in and between neurons and in extracellular media (concentrations of some substances like GABA and glutamate), and the involvement of specific brain regions. At present, there are several models partly reproducing certain features of the disease at different levels of detail.

A number of models were developed to test the hypotheses describing SWD initiation (onset of seizure) at the cellular level by simulation the dynamics of ion channels, the generation of action potentials under the influence of different concentration of various neurotransmitters. These models are described in detail in Destexhe (2014). Another class, so-called "lumped" models (Wendling, Benquet, Bartolomei, & Jirsa, 2016) approximate the activity of interacting cells populations, i.e. "lump" is an ensemble of a group of neurons which have a similar structure and function (Taylor & Baier, 2011). In such models, each population is modeled as a lumped oscillatory system described by several differential equations. For example, in Taylor et al. (2014) four ordinary differential equations (ODEs) were used: one for relay cells, one for interneurons, one for pyramidal cells and one for thalamo-cortical cells.

The model proposed in Suffczynski, Kalitzin, and Lopes da Silva F. (2004) is an advanced version of an much older model (Lopes da Silva, Hoeks, Smits, & Zetterberg, 1974), and is intermediate between the distributed neuronal network and lumped models, and it models the populations of interacting neurons integrating neuronal and network properties. The model consists of ODEs for transmembrane potentials and includes four cell types: two for the cortex and two for the thalamus (each type is modeled as a lumped system). In addition, specific properties of GABA were taken into account and sigmoid transfer functions were used. The transitions between the oscillatory and non-oscillatory regimes occur spontaneously, without changing the parameters of the system, due to its bistability.

Some authors have modeled in detail the role of GABA, one of the main neurotransmitters responsible for the occurrence of SWDs. In Destexhe and Sejnowski (1995) and Marten, Rodrigues, Benjamin, Richardson, and Terry (2009) the action of GABA is modeled by reaction–diffusion equations, and equations for the transmembrane potential. The model proposed in Chen et al. (2014) includes neurons of basal ganglia in addition to neurons of cortex and thalamus and demonstrates their bidirectional functional role in the onset and termination of absence seizures. In the Taylor et al. (2015), model the efficiency of SWD abatement by applying an external stimulus was studied. Liu, Wang, and Fan (2016) extended the Taylor model by introducing cortical inhibitory neurons. Finally, a phenomenological model of connected phase oscillators was proposed in Schmidt, Petkov, Richardson, and Terry (2014); it demonstrates transitions between different EEG-states such as transitions from the normal EEG to pathological SWDs.

The importance of the structure of a neural network for generation of SWDs is only at the beginning of being explored, although many authors assume that an intact cortico-thalamo-cortical network is imperative for SWD occurrence (Meeren, Veening, Möderscheim, Coenen, & van Luijtelaar, 2009). An important problem of the existing models is that all neurons of each structure generate an integrated signal that is transmitted to other structures, thereby simplifying connectivity between brain structures. However, actual neurons have individual projections to neurons of other structures, with being connected to some of them but not to all. At the same time, they may be not connected with nearby situated neurons of the same structure; an exception to the latter are neurons of the reticular thalamic nucleus, which are heavily interconnected. Therefore, the resulting network has a complex topology (see e.g. review Bullmore & Sporns, 2009), in which some neurons or small groups of them are important for the generation of SWDs due to the presence of effective feedback loops. The existence of such microcircuits was shown in Silberberg, Grillner, LeBeau, Maex, and Markram (2005). At the same time, there is the possibility that other neurons are not involved in the generation of SWDs or they are involved only passively. A large number of elements of a detailed network may lead to the emergence of fundamentally new effects which are not available in the "lumped" models, including effects important for the occurrence of SWDs. It is generally accepted that the generalized SWD are the result of synchronized firing of large number of neurons within and between brain structures (Snead, 1995). In addition, indeed, as has been shown in the relatively simple models, network topology can be essential to the synchronization of neurons (Belykh, de Lange, & Hasler, 2005). Differences in the structure of connections between neurons under normal and pathological conditions have not been studied largely, and have not been taken into account in existing approaches to generate SWDs using the same "lumped" model, which simulate a normal EEG, but with specifically selected parameters (Wendling, Bellanger, Bartolomei, & Chauvel, 2000). Similarly, in Breakspear et al. (2006) the bifurcation in the model of normal brain considered as an excitatory medium is studied for epilepsy modeling by choosing a special regime in which stationary wave exists.

Information about network structures in genetic rat models can be obtained from studies on coupling analysis from EEG or LFP (local field potentials) time series. In Meeren, Pijn, van Luijtelaar, Coenen, and Lopes da Silva (2002) the focal role of somatosensory cortex was established in WAG/Rij rats, one of the genetic absence models. In Lüttjohann and van Luijtelaar (2012) and Sysoeva, Lüttjohann, van Luijtelaar, and Sysoev (2016) the dynamics of involvement of different thalamic structures in the genesis (preictal to ictal to postictal) of SWDs was revealed. Propagation of SWDs over the cortex was studied in humans using MEG data in Westmijse, Ossenblock, Gunning, and van Luijtelaar (2009).

The aim of the present work is to describe a model which will reproduce the experimentally observed characteristics of SWDs and coupling, relying mainly on properties of hierarchically organized (oscillators are collected into groups corresponding to for absence epilepsy relevant brain structures) network of a large number of oscillators.

Each oscillator models a group of closely spaced and quasi identical neurons, with this group being smaller than any nucleus of the thalamus or layer of the somatosensory cortex Shayegh, Fattahi, Sadri, and Ansari-Asl, 2011). This approach has a tradition in electronics and is known as "large particles method" (Nordsieck, 1953). According to this approach, the electron beam in a traveling wave tube is modeled neither as a single bunch, nor as using the actual number of particles but as several dozens of nominal electrons. It allows taking into account the interactions between the individual units, and at the same time to carry out the numerical solution of equations of dynamics in a reasonable time.

2. Model

The developed model belongs to a class of mesoscale models, in which each "neuron" (also referred as "node" further) is actually a group of nearby situated neurons with a shared function. The model is organized into two levels.

The first (top) level consists of three compartments: an input layer representing the n.(ervus) trigeminus, the second element is a group of thalamic neurons (not divided into excitatory and inhibitory populations, therefore one cannot say what specific thalamic nucleus is modeled by this structure), and the third element, the somatosensory cortex. The somatosensory cortex is considered to contain the focal initiating zone with cortico-cortical, cortico-thalamic and thalamo-cortical interactions being critical for seizure initiation and development (Lüttjohann & van Luijtelaar, 2012; Meeren et al., 2002; Polack et al., 2007). The thalamus contains modulated relay cells. The n. trigeminus is a cranial nerve that provides tactile, proprioceptive, and nociceptive afference of the face to the dorsal thalamus and somatosensory cortex. This particular element is included into the model, since it has been shown that input from the peri-oral region and vibrissae is imperative for SWDs to occur since peripheral functional inactivation abolished all SWDs (Abbasova, Chepurnov, Chepurnova, & van Luijtelaar, 2010).

The second (low) level is the level of individual neurons belonging to one of the three modeled structures. Each neuron may be connected to other neurons in the model by the following rules:

1. N. trigeminus (external input) drives neurons of the thalamus,
2. thalamic neurons drive neurons of the somatosensory cortex,
3. cortical neurons drive other neurons of the somatosensory neocortex and neurons of thalamus.

An example of the model consisting of 43 neurons is shown in Fig. 1. In most cases, we used more neurons: 32 peripheral neurons, 60 thalamic neurons and 80 cortical neurons (172 in total).

FitzHugh–Nagumo equations (FitzHugh, 1955) (1) were used for modeling neurons of each type:

$$\begin{aligned} \frac{dx}{dt} &= x\,(a-x)\,(x-1) - y + \xi\,(t) \\ \frac{dy}{dt} &= bx - \gamma y \end{aligned} \tag{1}$$

with parameters $a = 0.8, b = 0.008, \gamma = 0.0033$, where ξ is white Gaussian noise.

The model of an individual neuron (1) used herein is much simpler than models proposed in the works of Destexhe, Babloyantz, and Sejnowski (1993) and Suffczynski et al. (2004), which took into account a variety of transmembrane currents, and in which numerous parameters were selected based on experimental results. Also, physico-chemical processes such as a role of specific excitatory and inhibitory neurotransmitter systems, as was done by Marten et al. (2009) were not included. Because of these simplifications, the proposed model is deprived of some specific properties of SWDs, but these simplifications might be instrumental to reveal clearly, what network architecture can provide by itself.

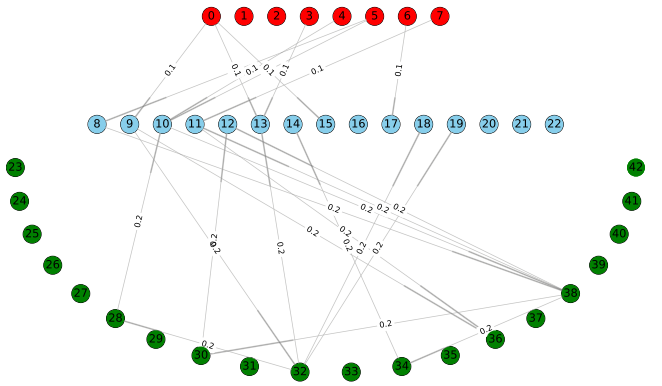

Fig. 1. Example of coupling architecture of the proposed model. The different colors show the different structures of neurons: red—peripheral, blue—thalamic neurons, green—neocortical neurons. Directed coupling is shown as lines; thickening at the end of the line corresponds to the direction of coupling. (For interpretation of the references to color in this figure legend, the reader is referred to the web version of this article.)

Couplings between the structures are arranged in a matrix C, in which row number corresponds to the driven neuron and the column number corresponds to the driving one. Coupling matrices were generated randomly by the following set of conditions: thalamic neurons receive inputs from n. trigeminus and project to neurons in the cortex. Cortical neurons are connected to several other cortical neurons and to neurons in the thalamus. The probability of occurrence of coupling depends on the structures involved: it was $0.5/N_e$, for elements of trigeminus to elements of thalamus, and $1/N$ in all other cases, where N is the number of neurons of the driving structure. The value of coupling coefficients (nonzero elements of C) was 0.1 for coupling from n. trigeminus to thalamus and 0.2 in all other cases. In principle, these values could be also randomized, but this would seriously complicate the management of the model to obtain the aimed behavior.

The equations of the network elements with couplings are represented by formula (2).

$$\begin{aligned} \frac{dx_i}{dt} &= x_i\,(a-x_i)\,(x_i-1) - y_i + \xi_i + \sum_{j\neq i} C_{i,j} h\left(x_j\,(t-\tau)\right), \\ \frac{dy_i}{dt} &= bx_i - \gamma y_i, \\ h\,(x) &= 1 + \frac{\tanh\,(x)}{2}. \end{aligned} \tag{2}$$

Time delay τ was selected for each matrix individually in a range from 5 to 15 units of time and it was the same for all the couplings within the same matrix. This value is close to physiologically meaningful values, but could be a little bit high. The model equations were solved numerically by Euler's method with step 0.5. Dimensionless unit of time was mapped to 1 ms, which corresponds to a conventional sampling rate of 2000 Hz. Similar sampling rate are typical for network signal analytical studies in animal models see, for example Lüttjohann and van Luijtelaar (2012), where sampling rate was equal to 2048 Hz.

Signals of individual nodes interictally (background activity) and during SWD-like discharges are shown in Fig. 2. Here and further under a transition to "seizure" or "discharge" in the model, we understand the relatively fast and significant (in 2 to 4 times) increase of amplitude of the signal, appearance of the pronounced shape and constant frequency about 8 Hz. At the individual node

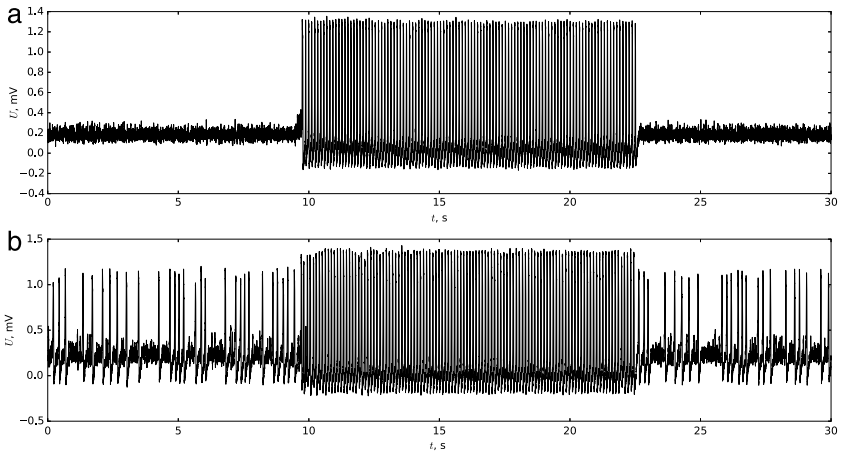

Fig. 2. The dynamics of individual neurons (a) not active preictally (b) active both inter and ictally. The epileptic discharge spontaneously began at 9.7 s and terminated spontaneously at 22.6 s. Since the neuron in the model represents a large number of nearby neurons, its oscillation amplitude cannot be compared straightly to amplitude measured in experiments.

level, this transition corresponds to the Andronov–Hopf bifurcation and synchronization of activity of many nodes. Since in the proposed model this transition is induced by the increase in the coupling from the n. trigeminus, we additionally demand that a real discharge has to last some (at least one or two) seconds after the stimulation removed, and finish spontaneously.[1] In most cases, the generation of spikes in the background was absent (see Fig. 2(a), there are subthreshold oscillations excited by noise). The periodic generation of the oscillations occurred during the discharge. Some neurons demonstrated non-periodic generation in the background and periodic one during the discharge—see Fig. 2(b).

The irregular interspike firing of neurons participating in absence seizures and their hyperpolarization during a seizure are in a good correspondence with the neurophysiological recordings of the hyperexcitable cells in the focal zone, reported in Depaulis and Charpier (2017) and Polack et al. (2007). One remark is necessary: in Depaulis and Charpier (2017) and Polack et al. (2007) the dynamics of individual neurons was measured, while our model reproduces the dynamics of a node, which is modeled as a single neuron, but at the same time it represents a group of nearby located neurons.

3. Results

3.1. Onset and termination of seizure

In total, more than 1000 coupling matrices were generated. Discharge initiation was carried by a smooth increase in the coupling coefficients between the n. trigeminus and the thalamus from the default value of 0.1 until the value 0.2 was reached, with a step size of 0.001 per 0.5 ms. Then, the value of 0.2 was held for 5 s. The decrease in coupling was symmetrical to the increase: 0.001 per time step (0.5 ms) from 0.2 until the original value 0.1 was reached. Time series were generated multiple times for each matrix using different noise realizations, while the level of noise being held constant; in each case an attempt to initiate a discharge was made. In addition to the signals of individual nodes, integrated signals from thalamus and cortex were obtained by summing the signals of individual nodes related to each structure. These signals were called "integrated" in the remainder of the paper; they correspond to the local field potentials measured experimentally.

[1] Please, consider that the amplitude of oscillations of a single node cannot be directly compared to the amplitude of unit activity measured experimentally, since the in the model represents a large number of nearby neurons.

In the proposed model an attempt to initiate the discharge could lead to one of four situations:

1. a discharge did not start; the model responded to the increase of the coupling coefficient by separate spikes in thalamus and cortex and by increasing the amplitude of the baseline subthreshold oscillations—see Fig. 3(a, e);
2. a discharge took place while the coupling coefficient between n. trigeminus and the thalamus was raised and stopped as soon as it returned to the normal value—see Fig. 3(b, f);
3. a discharge started and continued after the coupling coefficient between n. trigeminus and thalamus returned to the normal value, and then it finished spontaneously – see Fig. 3(c, g);
4. a discharge started and continued after the coupling coefficient between n. trigeminus and the thalamus returned to the normal value, but it did not finish spontaneously in the observation time—see Fig. 3(d, h).

Matrices, for which a discharge started and continued after the coupling coefficient between n. trigeminus and thalamus returned to the normal value, for at least some realizations of noise and ended spontaneously within the time of observation (situation 3), were considered as appropriate for modeling SWDs considering that most SWDs start and end within 5 to 15–30 s. In total, 10 such "absence" matrices were found. Ten fragments with the transition from normal to epileptiformic activity and back were generated for each of these matrices.

Modeled SWDs began suddenly, i.e. without a gradual increase in the amplitude of oscillations, and stopped suddenly. A sudden start and termination of SWDs are a main feature of SWDs, as has been established both in the clinic and in the genetic absence models based on visual inspection of the EEG (Coenen & van Luijtelaar, 2003). In the model this becomes possible partly due to noise.

Time series of modeled local field potentials of thalamus and cortex are shown in Fig. 4 together with the corresponding results of time frequency analysis (spectrograms). Many nodes of both cortex and thalamus started to show synchronous activity: we calculated phase synchronization index following (Allefeld & Kurths, 2004), and found it to be about 0.9–0.95 in all cases except nodes, which were not involved in the network's dynamics. The discharge begins from highly nonlinear oscillations with a main frequency of about 8.5 Hz (a first spike is well distinguishable). This frequency and its higher harmonics (17, 25.5 Hz) can be seen as yellow/orange

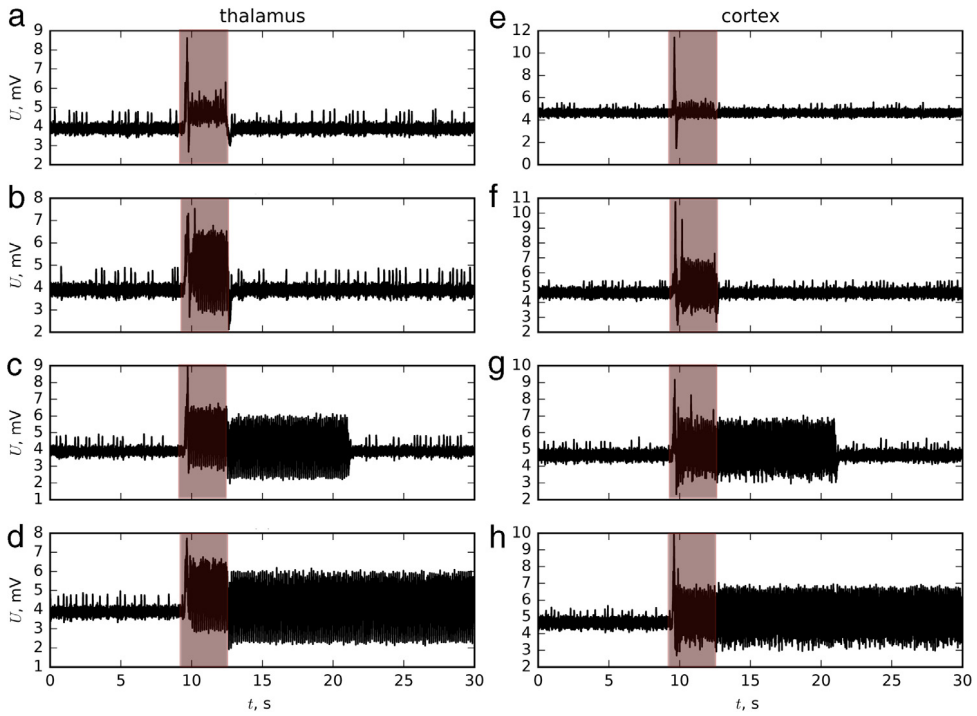

Fig. 3. Integrated neuronal signals (local field potentials) of thalamus (left column) and cortex (right column) in cases: (a, e)—a discharge did not start; (b, f)—periodic generation stopped with decreasing of the coupling coefficient between the n. trigeminus and the thalamus; (c, f)—a discharge started and finished spontaneously; (d, h)—a discharge started, but it did not finish in the observation time.

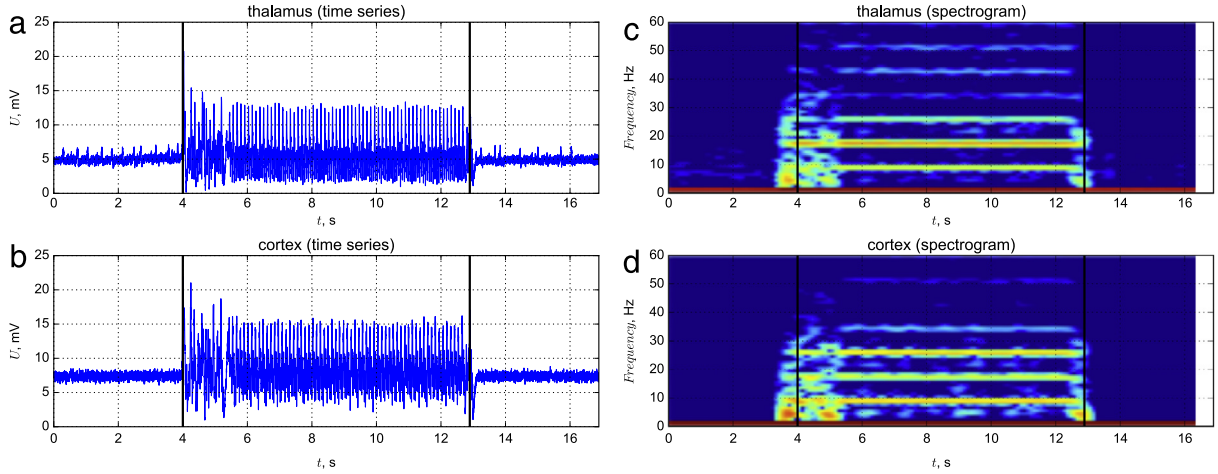

Fig. 4. Modeled signals of thalamus local field potentials (a), cortex (b) and the corresponding spectrograms—(c) and (d) respectively. For panel (c, d) the warmer the color, the higher is the power at the frequency: blue correspond to no power, while yellow and red—to the high power. (For interpretation of the references to color in this figure legend, the reader is referred to the web version of this article.)

lines during the seizure. The spectrogram of the model is very similar to the experimental spectrograms reported in Sysoeva, Lüttjohann et al. (2016). The first few seconds (while the increased coupling from the nervus trigeminus is present) are accompanied by a low-frequency component of about 4 Hz ($^1/_2$ subharmonic). The discharge onset depicted on the spectrogram appeared approximately 1 s earlier than on cortical and thalamic EEG (time series). Indeed, some oscillation at 8 Hz frequency appeared preictally, but they were small in amplitude. Delta and theta activity preceding the onset of SWD has been previously described in cortex and thalamus in the WAG/Rij absence model (van Luijtelaar et al., 2011). These oscillations are likely to be the result of coupling change, because usually a seizure starts 1–1.5 s after the actual change in coupling (Lüttjohann & van Luijtelaar, 2015; Sysoeva, Lüttjohann et al., 2016). But one has to keep in mind that the time resolution of the spectrogram in Fig. 4(c, d) is 1 s, so the spectrogram by itself is not enough and signal shape analysis is necessary to detect these oscillations, accompanied with spectral analysis with different time window length. The amplitude of the signal during the discharge was many times larger compared to the background activity, and signals became more regular, but not completely periodic. This may be due both to complex interactions in the network and the presence of noise and is in a good agreement with experimental results.

The ability of the model to generate SWD-like activity is based mainly on the structure of couplings. But an occurrence of SWD in each concrete case is probabilistic and depends on a concrete realization of the noise. To test this, 1000 realizations of noise were tested for each of 10 considered matrices with the same stimulus. The probability to get a "seizure" was found to be about 5%–7%

Table 1
Percentage of seizures remained after coupling removal.

Direction of coupling	Dynamics did not change	Discharge did not start	Discharge did not finish
nervus trigeminus → thalamus	83.1	14.5	2.4
thalamus → cortex	79.1	18.2	2.7
cortex → cortex	77.0	20.0	3.0
cortex → thalamus	87.5	11.6	0.9
Total	**83.0**	**15.0**	**2.0**

for matrices 1, 3, and 9, but about 0.1% for the matrix 2. For other matrices it was in between. The difference of this probability for different matrices matches the fact that for the well known genetic models of absence epilepsy (WAG/Rij rats) the probability of SWD occurrence is also different for different individuals, so it was even proposed to divide the animals into two sublines: A1–A1 (frequent seizures) and A2–A2 (seldom seizures) (Kalimullina, Musina, & Kuznetsova, 2013).

3.2. Stability of the model with respect to small variations in the structure of couplings

The model was tested for stability to small changes in the coupling matrix. For this purpose, links were removed from matrix one at a time (i.e. corresponding coupling coefficient was set to zero). Realizations of noise were fixed to provide the generation of normal appearing SWDs in the presence of the removed links. All of 10 found matrices were analyzed. The average percentage has been calculated for the three possible types of behavior (the results are summarized in Table 1):

1. discharge started and finished (dynamics did not change compared to the case before the removal of a link),
2. discharge did not start,
3. discharge did not finish.

As can be inferred from the data as presented in the Table 1, removal of a coupling did not lead to a change in behavior in most cases (83%), 15% of the couplings were critical to the initiation of discharge, and 2%—for its termination. This analysis shows that in the proposed model not all couplings are equal—the majority of them neither have any fundamental significance for the initiation of epileptiformic activity, nor for its termination. The earliest involvement or intracortical interaction into SWD initiation was found in experimental data analyzed by means of nonlinear correlation (Lüttjohann & van Luijtelaar, 2012) and Granger causality (Sysoeva, Lüttjohann et al., 2016). This means that at a first, not precise consideration, we can suppose that the whole network can be divided into 2 functional parts: an "epileptic" and a "normal" subnetwork. The "epileptic" subnetwork is relatively small (consists of 17% of all nodes), but very fragile, since elimination of any element of this network leads to an interruption of seizure activity. The "normal" subnetwork is not critical for the seizure's begin and termination but its nodes can participate in the seizures being involved and synchronized by elements of the "epileptic" subnetwork. The normal and robust part of brain that is modeled here might represent the network involved in processing sensory and motor information from periphery via thalamus to cortex and back to thalamus, and the thalamo-cortical network involved in the EEG signs of sleep, while the epileptic network is the same network but with additional connections. The fragility of this latter part of the network is abundantly backed up by experimental data from electrical stimulation studies in WAG/Rij and GAERS, showing that short (1 s) trains of low intensity cortical and subcortical 130 Hz stimulation during SWDs may quickly abort ongoing absences (Nelson et al., 2011; van Luijtelaar et al., 2011).

In order to test the hypothesis that the network can be divided into a "normal" and "epileptic" subnetwork, the effects of the removal of 2 links simultaneously were investigated. We reasoned as follows: if the separation of subnetworks is complete, synergetic couplings would not exist. Consequently: if the removal of 2 synergetic couplings prevent the occurrence of SWDs, and removal of each of them individually cannot, synergism will be demonstrated. All possible pairs of couplings, i.e. between thalamus and cortex in both directions, between cortical cells, and between n.trigeminus and thalamus, were examined. Since this is computationally intensive, only a single matrix was analyzed. In total, there were 6903 pairs of couplings. It was found that removal of 4089 pairs (59%) did not lead to a change in dynamics (the discharge started and finished), discharge did not start after removal of 2059 pairs (30%) and did not finish after removal of 755 pairs (11%). For the same matrix, the removal of one coupling led to the probability of disappearance of epileptiformic activity of 14%, and in 7% spontaneous abortion did not happen. To know, whether the results of removal of 2 couplings can be totally determined by results of removal of individual couplings (this supports the hypothesis of 2 separate subnetworks) or not, we had to make a probability analysis.

Let p_1, q_1 and r_1 denote probabilities of maintenance, elimination and non-completion of a discharge after removal of one coupling, and let p_2, q_2 and r_2 denote the same probabilities, but after removal of two couplings from the same matrix. Then, the following relation is valid:

$$1 = (p_1 + q_1 + r_1)^2 = p_1^2 + \left(q_1^2 + 2p_1q_1 + 2q_1r_1\right) + \left(r_1^2 + 2p_1r_1\right) = p_2 + q_2 + r_2. \quad (3)$$

Assuming that a synergetic effect is not present, discharges will continue to occur after removal of two couplings at once only if the discharges are maintained after separate removal of each coupling, i. e. $p_1^2 = p_2$. Discharges will not start after removal of two couplings if it does not start after removal at least one of them, i. e. $q_2 = q_1^2 + 2p_1q_1 + 2q_1r_1$. Discharges will not end after removal of two couplings at once, if it start and removal of at least one of the couplings leads to non-completion, i. e. $r_2 = r_1^2 + 2p_1r_1$. By the example of matrix 1: $p_1^2 = 0.79^2 = 0.6241$ that is slightly more than the actual $p_2 = 0.5923$; $q_1^2 + 2p_1q_1 + 2q_1r_1 = 0.2604$, that is less than the actual $q_2 = 0.3026$ and $r_1^2 + 2p_1r_1 = 0.1155$ that is close to the actual $r_2 = 0.1093$. Thus, the analysis showed that the number of pairs, removal of which leads to absence of discharge, is approximately 4% higher than it should be without synergetic effect. This value seems to be not very large, but this corresponds to an increase probability of preventing absence seizure from 26% to 30%, i.e. this probability becomes 1.16 times (+16%) larger. This also means that the separation of the network into an "epileptic" and "normal" subnetwork is far from complete, in agreement with the rarely investigated but widely spread assumption that spreading of SWDs after their cortical generation occurs via normal pathways involved in the transmission of sensory processes to the cortex and back to the thalamus or in modulating them (Kandel & Buzsáki, 1997) and in circuits generating the normal thalamo-cortical oscillations during sleep (Beenhakker & Huguenard, 2009). The latter authors proposed that absences seizures are hijacking the networks involved in normal thalamo-cortical oscillations, an idea that was earlier proposed by the Montreal group while studying the by penicillin induced transformation of sleep spindles to pathological SWD-like oscillations (Avoli, 2012).

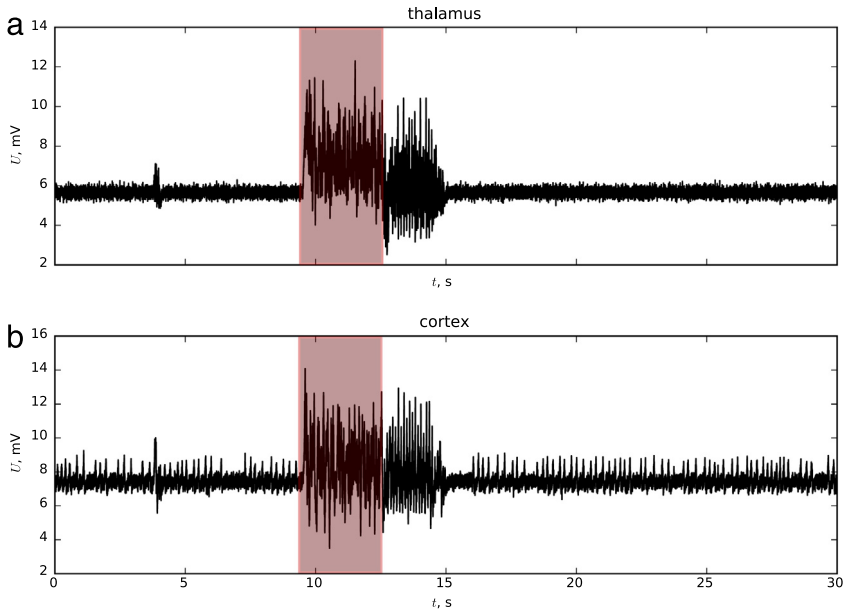

Fig. 5. Integral signal of model neurons of one structure (a time series of local field potentials) for matrices of double size (64 neurons of n. trigeminus, 120 neurons of the thalamus and 160 cortical neurons): (a)—time series of thalamic activity, (b)—time series of cortical activity.

3.3. Scalability of the model

Individual neurons of the model simulate a set of real neurons with similar characteristics. The closest analogy is the method of large particles in microwave electronics. If the analogy is correct and the model reflects the actual dynamics of epileptic network, it must demonstrate scaling: similar behavior should be observed at different levels of detail (different ratio of model neurons number to real number of neurons).

Results described in Sections 3.1 and 3.2 were obtained for models consisting of 172 neurons: 32 peripheral, 60 thalamic and 80 cortical neurons. A smaller number of neurons could not generate self-abortive spontaneously ending discharges in performed numerical experiments. Probably, this is due to insufficient network complexity. This behavior can be considered as normal for large particle models: there is always a minimum level of detail, subsequent roughening of the model leads to a loss of some of its major characteristics. A similar effect (complex behavior appears only at a large enough number of nodes) was described in Sompolinsky, Crisanti, and Sommers (1988) for their neuro-oscillatory model. For matrices of half size, it is not possible to get a stable generation of seizures. This became clear thanks to investigation of role of critical for link removal nodes in the Section 3.2: there must be many critical nodes with more than one link in each direction, those are not self-excitatory at the same moment (otherwise the matrix would be always generating), which is not possible for smaller networks.

Therefore, we doubled the number of neurons in each structure, and found a matrix which provides onset and termination of spontaneous discharges (see Fig. 5). In principle, even four times larger matrices also could be considered and investigated, but the number of links in such matrices makes the look for the suitable matrix very time consuming and laborious. Also, the analysis of the role of different nodes becomes complicated. Certainly, the increase of the number of neurons in the network leads to the appearance of new, additional effects, as well as complicates the search of the absence matrices.

3.4. Coupling analysis for simulated data

To compare the properties of the generated time series with the experimental signals of local field potentials, we tried to perform the same coupling analysis for the simulated data, as the analysis which was performed previously to the real ones in Sysoeva, Lüttjohann et al. (2016), Sysoeva, Sitnikova, and Sysoev (2016) and Sysoeva, Vinogradova, Kuznetsova, Sysoev, and van Rijn (2016). The main method used in these works was time variant adapted Granger causality (Sysoeva, Sitnikova, Sysoev, Bezruchko, & van Luijtelaar, 2014). Let us consider time series of two processes: the series $\{x_n\}_{n=1}^N$ from the process X, and the series $\{y_n\}_{n=1}^N$ from the other process Y, where N is a total length of the series. In our case, $\{x_n\}_{n=1}^N$ and $\{y_n\}_{n=1}^N$ are records of local field potentials.

First, to start with Granger causality, the model structure has to be established. Actually, one has to construct two models: the univariate (self-predicting) model for X based only on its own data, and bivariate (joint) model, including the data from the signal Y. In Sysoeva and Sysoev (2011) it was proposed to use an iterative map of the form (4) for the univariate model, the method of delays (Packard, Crutchfield, Farmer, & Shaw, 1980) for state vector reconstruction, and to use nonuniform embedding to take into account the main time scales and to reduce the dimension of the model.

$$x'_{n+\tau} = f\left(x_n, x_{n-l}, \ldots, x_{n-(D_s-1)l}\right) + \alpha_{Z_s+1} x_{n-l_T}, \tag{4}$$

$$f = \sum_{k=0}^{P} \sum_{q=1}^{C^k_{D_s+k}} \alpha_i^s \prod_{m=1}^{D_s} x_{n-(m-1)l}^{w^s_{k,\,m}}, \tag{5}$$

$$Z_s = C^P_{D_s+P},$$

$$\forall k = 0, \ldots, P \sum_{m=1}^{D_s} w^s_{k,\,m} = k,$$

where function f is a power polynomial of the degree P as proposed in Chen, Rangarajan, Feng, and Ding (2004), $C^k_{D_s+k}$ is the number of combinations from $(D_s + k)$ on k, x_n is a measured value at the time moment n, while x'_n is a value predicted by the model in the same time moment, D_s is the dimension (number of previous values used for the forecast), l—lag (time distance between the values used for the forecast), l_T—additional lag to account the main scale of oscillations, τ—forecast range, and also the coefficients $\alpha_i = 1, \ldots, Z_s + 1$, to be fitted by means of least squares routine. Let us denote the least-squares error of approximation as ϵ_s^2.

For a bivariate model, the similar structure (6) has to be implemented, since a bivariate model must contain the same terms dependent on x solely as in univariate.

$$x''_{n+\tau} = g\left(x_n, x_{n-l}, \ldots, x_{n-(D_s-1)l}, y_n\right) + \alpha_{Z_j+1} x_{n-l_T} + \alpha_{Z_j+2} y_{n-l_T} \tag{6}$$

$$\sum_{k=0}^{P} \sum_{q=1}^{C^k_{D_s+D_a+k}} \alpha_i^j \prod_{m=1}^{D_s} x_{n-(m-1)l}^{w^j_{k,\,\mathrm{m}}} \times \prod_{m=1}^{D_a} y_{n-(m-1)l}^{w^j_{k,(m+D_s)}}, \tag{7}$$

$$Z_j = C^P_{D_s+D_a+P},$$

$$\sum_{m=1}^{D_s+D_a} w^j_{k,\,\mathrm{m}} = k, \qquad \forall k = 0, \ldots, P$$

where g is another generalized polynomial function of the same order P as f, x''_n are values predicted by the bivariate model in time moment n (possibly different as from x'_n, as from x_n). Here, the only one previous value y_n from series of system Y was taken into account due to limitation of the amount of data. Let us denote the least-square error of prediction using model (6) as ϵ_j^2.

Such a structure was proved to be fine in comparison to many others in sense of ratio of sensitivity versus specificity (Kornilov, Medvedeva, Bezruchko, & Sysoev, 2016).

To determine the optimal model parameters: lag l and dimension D_s, the Bayesian information criterion (BIC, the minimum of the objective function (8)) was used according to Schwarz (1978). This criterion aims to reduce the number of coefficients in a model to make their estimates more reliable by introducing penalty.

$$s = \frac{N}{2} \ln \epsilon_s^2 + \frac{Z}{2} \ln N. \tag{8}$$

An analysis of the optimal values of the dimension D_s and polynomial order P showed that a linear model of large dimension suits well the background activity, whereas an empirical nonlinear model is required to describe the epileptiformic one. This seems to be in good correspondence with results of experimental data analysis reported in the appendix of Sysoeva, Lüttjohann et al. (2016).

Time series of model LFPs of the cortex and the thalamus were analyzed for interactions pair-wisely, i. e. they were considered as signals $\{x_n\}_{n=1}^N$ and $\{y_n\}_{n=1}^N$ and vice versa. The results were compared with previously obtained results from the experimental time series of local field potentials of WAG/Rij rats (Sysoeva, Lüttjohann et al., 2016; Sysoeva, Sitnikova et al., 2016). The analysis was performed in a time window, as proposed in Hesse, Molle, Arnold, and Schack (2003). Window width of 0.5 s (1000 values) was used with a shift between windows equal to 0.1 s—parameters that are very similar to those in Sysoeva, Lüttjohann et al. (2016). The analysis was also performed similarly to Sysoeva, Lüttjohann et al. (2016). Onsets and terminations of all the model seizures were combined. Background level of coupling was established using intervals 10–7 s before the appearance of the generalized SWD, i.e. seizure onset. Resulting values of prediction improvement were averaged first over individual discharges for each matrix (a matrix was collated to an animal), then—over all the matrices, given the normalized values. The mean values obtained for an each time point for each matrix were considered as an ensemble, and their average was tested for significant difference from the background level.

These dependencies are shown in Fig. 6. They well reproduce dependencies obtained in an earlier study (Sitnikova, Dikanev, Smirnov, Bezruchko, & van Luijtelaar, 2008) (the coupling is increase all over the seizure in comparison to the baseline), but also exhibit an increase in preictal coherence, as was shown in real data from WAG/Rij rats (Sysoeva, Lüttjohann et al., 2016).

4. Conclusion and discussion

4.1. Proposed model among the models of epilepsy

Existing models of absence epilepsy focus mainly on modeling the results of neurochemical and bioelectrical measurements in individual neurons of somatosensory cortex and different parts of the thalamus and in the surrounding pericellular space. The SWDs in those models arise from the interaction of a small (for example, four in Suffczynski et al. (2004)) number of oscillatory models of individual neurons. Thus, the occurrence of epileptiformic activity is either the result of a change of model parameters (Wendling et al., 2000), or switching between attractors (Suffczynski et al., 2004) in a relatively low-dimensional system.

At the same time, systems consisting of a large number of elements may show complex behavior, even if the individual elements can only show simple regular regimes (Kuramoto & Battogtokh, 2002), given that elements are identical and coupling function is the same (Sompolinsky et al., 1988). The main mechanism of complex behavior of such networks is the result of a specific coupling architecture of a large number of elements. The question of couplings architecture influence on absence discharges generation is studied well at the level of functional brain structures (Lüttjohann & van Luijtelaar, 2012; Meeren et al., 2002). Nevertheless, it is less clear what happens at the level of interaction between individual neurons. Existing methods for measuring the signals of individual motor units do not provide an opportunity to measure the time series of electrical activity of a large (at least about one hundred) number of neurons in the brain from various leads of cortex and/or thalamus at the same time. Therefore, we suppose that modeling SWDs by large networks of oscillators is a promising approach to study SWDs mechanisms, if the time series can reproduce properties of signals measured in experiments.

Currently, there is no clear evidence of whether the mechanisms of absence activity are common in all cases, or the generation of SWDs may be caused by various factors. Known is, than an intact cortico-thalamo-cortical network is a prerequisite for SWDs to occur since all functional deactivation studies (lesions) of the various constituent elements show that SWD no longer occur (Meeren et al., 2009; Polack et al., 2007; Scicchitano, van Rijn, & van Luijtelaar, 2015; Sitnikova & van Luijtelaar, 2004). Here we formulate the hypothesis that one of the most important criteria for the possibility of generating SWDs is a specific pathological architecture of couplings in the brain at the level of individual neurons in a network consisting of a large number of neurons. This architecture can occur because of random and harmless in other sense mutations or by a combination of genes of the parents. In the commonly used genetic models of absence epilepsy (WAG/Rij and GAERS rats) this pathological architecture has been fixed by inbreeding or selection. At the same time, a pathological architecture of couplings may not differ significantly from non-pathological one in terms of average indicators of network (the average number of couplings, the network's complexity). However, the presence of a sufficient number of specific feedback loops at the level of interaction between individual neurons leads to the possibility of switching the entire network from a normal regime to a pathological one. Moreover, this pathological regime is also stable or metastable, i. e. it represents a long transition process, during which the amplitude–frequency characteristics of the signals are approximately preserved.

Thus, the proposed model is neither intended to replace the existing models of absence epilepsy; nor it denies the results obtained at the cellular level and the level of the large structures of the brain (interaction thalamus ↔ somatosensory cortex). It shows that the transition to pathological behavior is possible due to the specifics of the network properties of a large number individually interacting neurons.

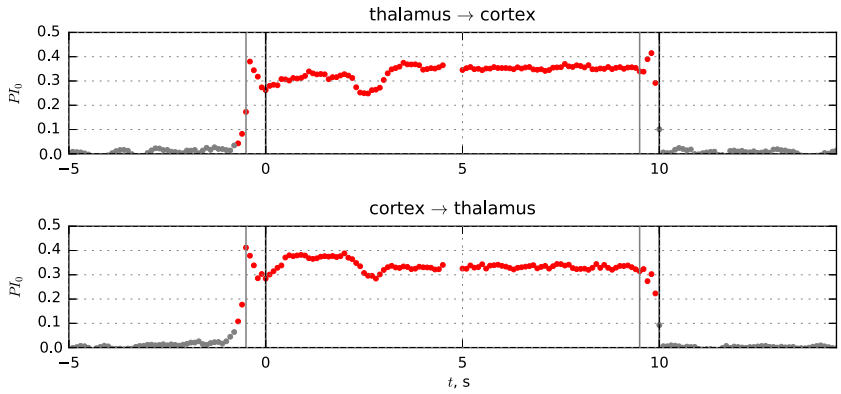

Fig. 6. Dependence of prediction improvement from the time for model discharges.

4.2. Coupling analysis

By now, significant progress has been made in the area of coupling analysis between structures of the brain in the onset and maintenance of SWDs (Lüttjohann & van Luijtelaar, 2012; Sysoeva, Lüttjohann et al., 2016; Sysoeva, Vinogradova et al., 2016). At the same time, it is not clear whether existing models can adequately reproduce these results if the signals generated by them are analyzed by the methods similar to the ones used for experimental data. The problem can be formulated as follows. From the one hand, there are models of SWDs, constructed from first principles, in which coupling is set based on physiological studies. From the other hand, there are results of coupling estimation from experimentally measured signal, also leading to some coupling architecture. But these two approaches are still in bad correspondence. E. g. there were no attempt to reconstruct the models of SWDs build so far from the measured time series. The model constructed in this paper takes the first step: it reproduces the increase of coupling in preictal phase, detected by different methods (Granger causality and nonlinear correlation) on various LFP data.

Interactions obtained in our model system as described in the Section 3.4 are most similar to the interaction of the somatosensory cortex and the caudal part of the reticular nucleus of the thalamus, as was established in WAG/Rij rats. These channels pairs were important for maintaining the discharge (Sysoeva, Lüttjohann et al., 2016). Therefore, the interaction starts slightly earlier than the onset of the discharge and remains increased throughout the ictal period. It looks quite logical that in the presence of only two hypothetical structures of the brain, the pair responsible for maintaining the discharge is necessarily required.

Couplings between the individual layers of the somatosensory cortex are responsible for the SWD initiation process in WAG/Rij rats (Lüttjohann & van Luijtelaar, 2012; Sysoeva, Lüttjohann et al., 2016) and between cells in different cortical layers in GAERS (Polack, Mahon, Chavez, & Charpier, 2009). That is what our model demonstrates: removal of intracortical interaction may prevent SWD occurrence.

4.3. Main capabilities of the model

The model reproduces the main features of the transition from normal activity to the epileptiformic one and vice versa:

- an increase in the amplitude of oscillations,
- the emergence of the main frequency (about 8 Hz for the rat-models), its higher harmonics (simultaneously oscillations become more non-linear, and their dimension reduces),
- almost sudden switching from a normal to pathologic activity and vice versa,
- synchronization both between individual cells and between large structures (areas of the somatosensory cortex and the nuclei of the thalamus),
- the ability to generate trains of seizures.

At the same time, the model also partly reproduces an important feature of evolution of couplings found in recent studies (Lüttjohann & van Luijtelaar, 2012; Sysoeva, Lüttjohann et al., 2016)—preictal growth of coupling (in the model to 0.8–0.9, in an experiment from 3.5 to 0.5 in different pairs of channels).

In the proposed model, individual neurons could start to fire in a pathological regime while being silent in a normal one. However, it is also possible that neurons were active interictally or preictally, so in a normal regime, and they became synchronized with other neurons at the transition to seizure activity. The experiments give contradictory results: there were no silent cells during the generation of SWDs in thalamus and somatosensory cortex in neuroleptic anesthetized WAG/Rij rats (Staak & Pape, 2001), however other studies have shown that 60% of the network cells can be silent (Crunelli & Leresche, 2002) during SWDs. The question of what behavior is more typical, has not yet been solved experimentally, as described in Suffczynski et al. (2004), but it is important that the model is able to reproduce both situations.

The model showed ability for scaling: the possibility of generating pathological activity is preserved, with doubling the number of model neurons. We believe this ability to be important, because following our "large particles" approach we suggest that the exact number of nodes is not of great importance, but model can work starting from a reasonably large number of nodes until the size of model becomes too large for a mesoscale model, so many other, microscopic effects have to be taken into account.

The model demonstrates that different couplings can have different effects on the ability to transit to epileptiformic activity. Although all neurons were involved into epileptiformic activity, in 83% of cases removal of one coupling and in 59% of two couplings did lead to a change in firing regime. Only 15% of the couplings were critical for initiation and maintenance of the activity and only 2%—for its termination. The links critical for seizure initiation have some specifics: the number of links in the model connected to each node varied from 1 to 7, but some nodes occurred to be most critical: those having 2 incoming and 2 outcoming connections, with at least one connection to the cortex and one back. From these nodes, 100% were critical for initiation, and these nodes participated in ≈70% of total number of links leading to stop of initiation. At the same time, nodes with more connections, e. g. 6 in total, were more stable: they had to many links, so a removal of a single link was usually not important. Nodes with less links are also not so important, since they are not participating actively in thalamo-cortical feedback loops.

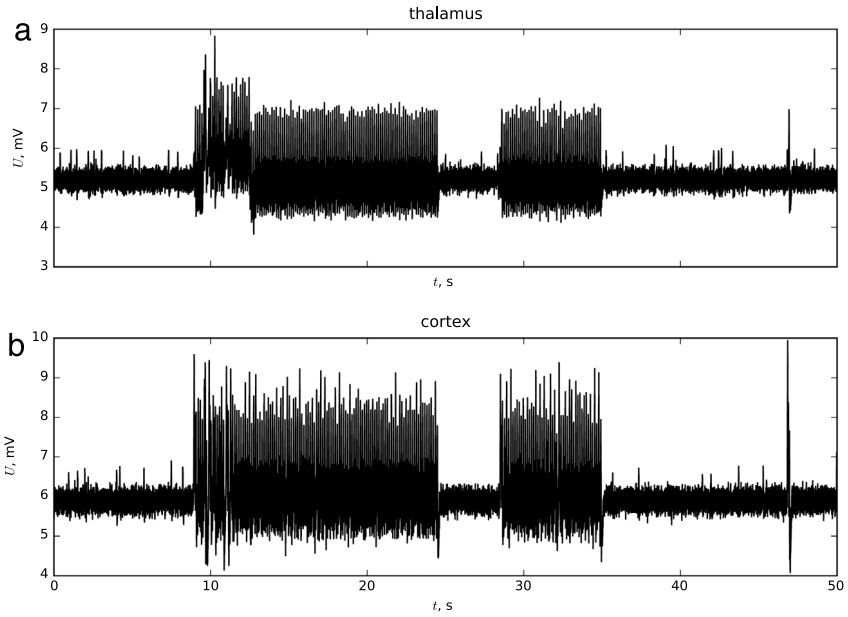

Fig. A.7. An absence discharge with a spontaneous restart (an example of "seizure train").

At the same time, the model demonstrates synergistic effect of couplings: removal of 4% pairs of couplings eliminated the possibility of generating SWDs, while the removal of each of these couplings individually did not lead to that effect. This means that the network cannot be completely separated into two subnetworks: one responsible for seizure activity, and the other, responsible for "normal" activity and participating in seizures only passively.

The importance of the delay in coupling (time needed for signal propagation) for SWD generation is not quite clear yet. The proposed model basically works only in presence of a small delay (5–15 ms). Undoubtedly, in a real brain there are also delays between structures, being caused primarily by signal transmission through the chemical synapses, and the propagation time along the axon (real delay could be smaller). But it is not clear, what impact such a delay could have on the generation of SWDs.

4.4. Limitations of the proposed model

The model has a number of limitations. The main source of these limitations is that simplified FitzHugh–Nagumo equations were used for modeling individual nodes. It does not take into account the different ion channels and the role of neurotransmitters systems, e.g. ionotropic and metabotropic glutamate and GABA receptors. Moreover, interactions between neurons are not divided into excitatory and inhibitory. As a result, the waveform does not reproduce the typical shape of SWDs (Sargsyan, Sitnikova, Melkonyan, Mkrtchian, & van Luijtelaar., 2007).

The model uses a simplified scheme of the organization of brain cells. Only three compartments were modeled: the input via the n. trigeminus, and the thalamus reciprocally connected to the cortex. Different nuclei of the thalamus and different types of cells in the different layers of the cortex have a different and complex functional organization, which simulates in the model only partly due to the couplings between cortical neurons.

The model depends on initiation of the discharges by the n. trigeminus, which models efferents of the vibrissae and peri oral area of the skin (Abbasova et al., 2010; Sitnikova, 2000). There is no reason to believe that this is the only factor involved in triggering SWDs. In some cases, the model is able to generate spontaneous discharges by switching from normal activity to an oscillatory mode (epileptiformic activity) due to noise. Interestingly, this was more likely to occur for the model with a double number of nodes, as was considered in Section 3.3.

The foregoing limitations necessarily arise, because otherwise the construction of a model would have been too difficult for the single study. We also tried to make the model as simple as possible to find what effects could be obtained by means of the hierarchical network. Including many additional differences in nodes and links would contaminate this evidence.

Acknowledgments

Authors are grateful to the late Prof. Galina D. Kuznetsova from the Institute of Higher Nervous Activity and Physiology of RAS for fruitful discussions and support. She left this world in January 2017, so we devote this study to her memory.

The work was supported by Russian Foundation for Basic Research, Grant 17-02-00307, DAAD Mikhail Lomonosov program, Linie B, personal funding reference number 57320204 (19.10004.2017/ЛААД), and Stipendium of President of Russian Federation for support of young scientists СП-1510.2015.4.

Appendix A. Trains of seizures

It has been noticed that the absence seizures often come one after another with a minor interval (Midzyanovskaya, Strelkov, van Rijn, Budziszewska, van Luijtelaar, & G., 2006). The mechanism of this phenomenon is not well understood, but it is shown that the probability of finding a new discharge immediately after the previous one is significantly higher than that after a long period of normal activity (Bosnyakova et al., 2007). The proposed model is not able to reproduce the distribution of the intervals observed in the experiment as it is a model of a single discharge. However, for some of the matrices, trains of seizures (short interval between the first and second part of discharge) occurred to be possible after a single initiation. An example of such a discharge is given in Fig. A.7. The ability to generate the trains of seizures is a feature of coupling architecture in the matrix, since one considered matrix (number 7) was able to generate them in 3 cases of 34 considered, while other 9 matrices were not.

Appendix B. Supplementary data

Supplementary material related to this article can be found online at http://dx.doi.org/10.1016/j.neunet.2017.12.002.

References

Abbasova, K., Chepurnov, S., Chepurnova, N., & van Luijtelaar, G. (2010). The role of perioral afferentation in the occurrence of spike-wave discharges in the WAG/Rij model of absence epilepsy. *Brain Research*, *1366*, 257–262.

Allefeld, C., & Kurths, J. (2004). Testing for phase synchronization. *International Journal of Bifurcation and Chaos*, *14*, 405–416. http://dx.doi.org/10.1142/S0218127404009051X.

Avoli, M. (2012). A brief history on the oscillating roles of thalamus and cortex in absence seizures. *Epilepsia*, *53*, 779–789.

Beenhakker, M., & Huguenard, J. (2009). Neurons that fire together also conspire together: is normal sleep circuitry hijacked to generate epilepsy? *Neuron*, *62*, 612–632. http://dx.doi.org/10.1016/j.neuron.2009.05.015.

Belykh, I., de Lange, E., & Hasler, M. (2005). Synchronization of Bursting Neurons: What Matters in the Network Topology. *Physical Review Letters*, *94*(18), 188101. http://dx.doi.org/10.1103/PhysRevLett.94.188101.

Berg, A., Levy, S., Testa, M., & Blumenfeld, H. (2014). Long-term seizure remission in childhood absence epilepsy: might initial treatment matter. *Epilepsia*, *55*(4), 551–557. http://dx.doi.org/10.1111/epi.12551.

Bosnyakova, D., Gabova, A., Zharikova, A., Gnezditski, V., Kuznetsova, G., & van Luijtelaar, G. (2007). Some peculiarities of time-frequency dynamics of spike-wave discharges in humans and rats. *Clinical Neurophysiology*, *118*(8), 1736–1743. http://dx.doi.org/10.1016/j.clinph.2007.04.013.

Breakspear, M., Roberts, J. A., Terry, J. R., Rodrigues, S., Mahant, N., & Robinson, P. A. (2006). A unifying explanation of primary generalized seizures through nonlinear brain modeling and bifurcation analysis. *Cerebral Cortex*, *16*(9), 1296–1313. http://dx.doi.org/10.1093/cercor/bhj072.

Bullmore, E., & Sporns, O. (2009). Complex brain networks: graph theoretical analysis of structural and functional systems. *Nature Reviews Neuroscience*, *10*, 186–198. http://dx.doi.org/10.1038/nrn2575.

Chen, M., Guo, D., Wang, T., Jing, W., Xia, Y., & Xu, P. (2014). Bidirectional control of absence seizures by the Basal Ganglia: a computational evidence. *PLoS Computational Biology*, *10*(3), 1–17. http://dx.doi.org/10.1371/journal.pcbi.1003495.

Chen, Y., Rangarajan, G., Feng, J., & Ding, M. (2004). Analyzing multiple nonlinear time series with extended granger causality. *Physics Letters A*, *324*(1), 26–35. http://dx.doi.org/10.1016/j.physleta.2004.02.032.

Coenen, A., & van Luijtelaar, G. (2003). Genetic animal models for absence epilepsy: a review of the WAG/Rij strain of rats. *Behav Genetics*, *33*, 635–655. http://dx.doi.org/10.1023/A:1026179013847.

Crunelli, J., & Leresche, N. (2002). Childhood absence epilepsy: genes, channels, neurons and networks. *Nature Reviews Neuroscience*, *3*, 371–382. http://dx.doi.org/10.1038/nrn811.

Depaulis, A., & Charpier, S. (2017). Pathophysiology of absence epilepsy: Insights from genetic models. *Neuroscience Lette*. http://dx.doi.org/10.1016/j.neulet.2017.02.035.

Destexhe, A. (2014). Network models of absence seizures, . (pp. 11–35), http://dx.doi.org/10.1016/B978-0-12-415804-7.00002-2.

Destexhe, A., Babloyantz, A., & Sejnowski, T. (1993). Ionic mechanisms for intrinsic slow oscillations in thalamic relay neurons. *Biophysical Journal*, *65*(4), 1538–1552. http://dx.doi.org/10.1016/S0006-3495(93)81190-1.

Destexhe, A., & Sejnowski, T. (1995). G protein activation kinetics and spillover of gamma-aminobutyric acid may account for differences between inhibitory responses in the hippocampus and thalamus. *Proceedings of the National Academy of Sciences of the United States of America*, *92*, 9515–9519.

FitzHugh, R. (1955). Mathematical models of threshold phenomena in the nerve membrane. *Bulletin of Mathematical Biophysics*, *17*, 257–269. http://dx.doi.org/10.1007/BF02477753.

Hesse, R., Molle, E., Arnold, M., & Schack, B. (2003). The use of time-variant EEG Granger causality for inspecting directed interdependencies of neural assemblies. *Journal of Neuroscience Methods*, *124*, 27–44. http://dx.doi.org/10.1016/S0165-0270(02)00366-7.

Inoue, M., Duysens, J., Vossen, J., & Coenen, A. (1993). Thalamic multiple-unit activity underlying spike-wave discharges in anesthetized rats. *Brain Research*, *612*(1–2), 35–40. http://dx.doi.org/10.1016/0006-8993(93)91641-5.

Kalimullina, L., Musina, A., & Kuznetsova, G. (2013). experimental approaches to studies of the role of the genotype at the TAG 1A locus of the dopamine D2 receptor in epileptogenesis. *Neuroscience and Behavioral Physiology*, *43*(8), 935–940. http://dx.doi.org/10.1007/s11055-013-9831-z.

Kandel, A., & Buzsáki, G. (1997). Cellular-synaptic generation of sleep spindles, spike-and-wave discharges, and evoked thalamocortical responses in the neocortex of the rat. *Journal of Neuroscience*, *17*, 6783–6797.

Kornilov, M., Medvedeva, T., Bezruchko, B., & Sysoev, I. (2016). Choosing the optimal model parameters for Granger causality in application to time series with main timescale. *Chaos, Solitons & Fractals*, *82*, 11–21. http://dx.doi.org/10.1016/j.chaos.2015.10.027.

Kuramoto, Y., & Battogtokh, D. (2002). Coexistence of coherence and incoherence in nonlocally coupled phase oscillators. *Nonlinear Phenomena in Complex Systems*, *5*(4), 380–385.

Liu, S., Wang, Q., & Fan, D. (2016). Disinhibition-induced delayed onset of epileptic spike-wave discharges in a five variable model of cortex and thalamus. *Frontiers in Computational Neuroscience*, *10*. http://dx.doi.org/10.3389/fncom.2016.00028.

Lopes da Silva, F., Hoeks, A., Smits, H., & Zetterberg, L. (1974). Model of brain rhythmic activity: the alpha-rhythm of the thalamus. *Kybernetic*, *15*, 27–37. http://dx.doi.org/10.1007/BF00270757.

Lüttjohann, A., & van Luijtelaar, G. (2012). The dynamics of cortico-thalamo-cortical interactions at the transition from pre-ictal to ictal LFPs in absence epilepsy. *Neurobiology of Disease*, *47*, 47–60. http://dx.doi.org/10.1016/j.nbd.2012.03.023.

Lüttjohann, A., & van Luijtelaar, G. (2015). Dynamics of networks during absence seizure's on- and offset in rodents and man. *Frontiers in Physiology*, *6*, 16. http://dx.doi.org/10.3389/fphys.2015.00016.

Marescaux, C., Vergnes, M., & Depaulis, A. (1992). Genetic absence epilepsy in rats from Strasbourg - a review. *Journal of Neural Transmission Supplementa*, *35*, 37–69. http://dx.doi.org/10.1007/978-3-7091-9206-1_4.

Marten, F., Rodrigues, S., Benjamin, O., Richardson, M., & Terry, J. (2009). Onset of polyspike complexes in a mean-field model of human electroencephalography and its application to absence epilepsy. *Philosophical Transactions of the Royal Society A*, *367*, 1145–1161. http://dx.doi.org/10.1098/rsta.2008.0255.

Meeren, H., Pijn, J., van Luijtelaar, G., Coenen, A., & Lopes da Silva, F. (2002). Cortical focus drives widespread corticothalamic networks during spontaneous absence seizures in rats. Journal of Neuroscience. *Ournal of Neuroscience*, *22*, 1480–1495.

Meeren, H., Veening, J., Möderscheim, T., Coenen, A., & van Luijtelaar, G. (2009). Thalamic lesions in a genetic rat model of absence epilepsy: dissociation between spike-wave discharges and sleep spindles. *Experimental Neurology*, *217*, 25–37. http://dx.doi.org/10.1016/j.expneurol.2009.01.009.

Midzyanovskaya, I., Strelkov, V., van Rijn, C., Budziszewska, B., & van Luijtelaar, G. K. G. (2006). Measuring clusters of spontaneous spike-wave discharges in absence epileptic rats. *Journal of Neuroscience Methods*, *154*(1–2), 83–89. http://dx.doi.org/10.1016/j.jneumeth.2005.12.014.

Moeller, F., LeVan, P., Muhle, H., Stephani, U., Dubeau, F., Siniatchkin, M., et al. (2010). Absence seizures: individual patterns revealed by EEG-fMRI. *Epilepsia*, *51*, 2000–2010. http://dx.doi.org/10.1111/j.1528-1167.2010.02698.x.

Nelson, T., Suhr, C., Freestone, D., Lai, A., Halliday, A., McLean, K., et al. (2011). Closed-loop seizure control with very high frequency electrical stimulation at seizure onset in the GAERS model of absence epilepsy. *International Journal of Neural Systems*, *21*, 163–173. http://dx.doi.org/10.1142/S0129065711002717.

Nordsieck, A. (1953). Theory of the large signal behavior of traveling-wave amplifiers. *Proceedings IRE*, *41*(5), 630–637. http://dx.doi.org/10.1109/JRPROC.1953.274404.

Packard, N., Crutchfield, J., Farmer, J., & Shaw, R. (1980). Geometry from a time series. *Physical Review Letters*, *45*, 712–716. http://dx.doi.org/10.1103/PhysRevLett.45.712.

Panayiotopoulos, C. P. (2001). Treatment of typical absence seizures and related epileptic syndromes. *Paediatric Drugs*, *3*(5), 379–403. http://dx.doi.org/10.2165/00128072-200103050-00006.

Polack, P., Guillemain, I., Hu, E., Deransart, C., Depaulis, A., & Charpier, S. (2007). Deep layer somatosensory cortical neurons initiate spike-and-wave discharges in a genetic model of absence seizures. *Journal of Neuroscience*, *27*, 6590–6599. http://dx.doi.org/10.1523/JNEUROSCI.0753-07.2007.

Polack, P., Mahon, S., Chavez, M., & Charpier, S. (2009). Inactivation of the somatosensory cortex prevents paroxysmal oscillations in cortical and related thalamic neurons in a genetic model of absence epilepsy. *Cerebral Cortex*, *19*, 2078–2091. http://dx.doi.org/10.1093/cercor/bhn237.

Sadleir, L., Farrell, K., Smith, S., et al. (2006). Electroclinical features of absence seizures in childhood absence epilepsy. *Neurology*, *67*(3), 413–418. http://dx.doi.org/10.1212/01.wnl.0000228257.60184.82.

Sargsyan, A., Sitnikova, E., Melkonyan, A., Mkrtchian, H., & van Luijtelaar., G. (2007). Simulation of sleep spindles and spike and wave discharges using a novel method for the calculation of field potentials in rats. *Journal of Neuroscience Methods*, *164*, 161–176. http://dx.doi.org/10.1016/j.jneumeth.2007.03.023.

Schmidt, H., Petkov, G., Richardson, M., & Terry, L. (2014). Dynamics on networks: the role of local dynamics and global networks on the emergence of hypersynchronous neural activity. *PLoS Computational Biology*. http://dx.doi.org/10.1371/journal.pcbi.1003947.

Schwarz, G. (1978). Estimating the dimension of a model. *The Annals of Statistics*, *6*(2), 461–464. http://dx.doi.org/10.1214/aos/1176344136.

Scicchitano, F., van Rijn, C., & van Luijtelaar, G. (2015). Unilateral and bilateral cortical resection: effects on spike-wave discharges in a genetic absence epilepsy model. *PLoS One*, *10*(8), . http://dx.doi.org/10.1371/journal.pone.0133594.

Shayegh, F., Fattahi, R., Sadri, S., & Ansari-Asl, K. (2011). A brief survey of computational models of normal and epileptic eeg signals: A guideline to model-based seizure prediction. *Journal of Medical Signals and Sensors*, *1*, 62–72.

Silberberg, G., Grillner, S., LeBeau, F., Maex, R., & Markram, H. (2005). Synaptic pathways in neural microcircuits. *Trends in Neurosciences*, *28*, 541–551. http://dx.doi.org/10.1016/j.tins.2005.08.004.

Sitnikova, E. (2000). Vibrissectomy in rats in early ontogeny leads to disordered functional properties of the cortical projection neurons. *Zh Vyssh Nerv Deiat Im I P Pavlova*, *50*(1), 137–141.

Sitnikova, E., Dikanev, T., Smirnov, D., Bezruchko, B., & van Luijtelaar, G. (2008). Granger causality: cortico-thalamic interdependencies during absence seizures in WAG/Rij rats. *Journal of Neuroscience Methods*, *170*(2), 245–254. http://dx.doi.org/10.1016/j.jneumeth.2008.01.017.

Sitnikova, E., & van Luijtelaar, G. (2004). Cortical control of generalized absence seizures: effect of lidocaine applied to the somatosensory cortex in WAG/Rij rats. *Brain Research*, *1012*(1–2), 127–137. http://dx.doi.org/10.1016/S0006-8993(04)00510-4.

Sitnikova, E., & van Luijtelaar, G. (2007). Electroencephalographic characterization of spike-wave discharges in cortex and thalamus in WAG/Rij rats. *Epilepsia*, *48*, 2296–2311. http://dx.doi.org/10.1111/j.1528-1167.2007.01250.x.

Snead, O. (1995). Basic mechanisms of generalized absence seizures. *Annals of Neurology*, *37*, 146–157. http://dx.doi.org/10.1002/ana.410370204.

Sompolinsky, H., Crisanti, A., & Sommers, H. (1988). Chaos in random neural networks. *Physical Review Letters*, *61*(3), 259–262. http://dx.doi.org/10.1103/PhysRevLett.61.259.

Staak, R., & Pape, H. (2001). Contribution of GABAA and GABAB receptors to thalamic neuronal activity during spontaneous absence seizures in rats. *Journal of Neuroscience*, *21*, 1378–1384.

Suffczynski, P., Kalitzin, S., & Lopes da Silva F., H. (2004). Dynamics of non-convulsive epileptic phenomena modeled by a bistable neuronal network. *Neuroscience*, *126*, 467–484. http://dx.doi.org/10.1016/j.neuroscience.2004.03.014.

Sysoeva, M., Lüttjohann, A., van Luijtelaar, G., & Sysoev, I. (2016). Dynamics of directional coupling underlying spike-wave discharges. *Neuroscience*, *314*, 75–89. http://dx.doi.org/10.1016/j.neuroscience.2015.11.044.

Sysoeva, M., Sitnikova, E., & Sysoev, I. (2016). Thalamo-cortical mechanisms of initiation, maintenance and termination of spike-wave discharges at WAG/Rij rats. *Zh Vyssh Nerv Deiat Im I P Pavlova*, *66*(1), 103–112.

Sysoeva, M., Sitnikova, E., Sysoev, I., Bezruchko, B., & van Luijtelaar, G. (2014). Application of adaptive nonlinear Granger causality: Disclosing network changes before and after absence seizure onset in a genetic rat model. *Journal of Neuroscience Methods*, *226*, 33–41. http://dx.doi.org/10.1016/j.jneumeth.2014.01.028.

Sysoeva, M., & Sysoev, I. (2011). Mathematical modeling of encephalogram dynamics during epileptic seizure. *Technical Physics Letters*, *38*(2), 151–154. http://dx.doi.org/10.1134/S1063785012020137.

Sysoeva, M., Vinogradova, L., Kuznetsova, G., Sysoev, I., & van Rijn, C. (2016). Changes in corticocortical and corticohippocampal network during absence seizures in WAG/Rij rats revealed with time varying Granger causality. *Epilepsy and Behavior*, *64*, 44–50. http://dx.doi.org/10.1016/j.yebeh.2016.08.009.

Taylor, P., & Baier, G. (2011). A spatially extended model for macroscopic spike-wave discharges. *Journal of Computational Neuroscience*, *31*, 679–684. http://dx.doi.org/10.1007/s10827-011-0332-1.

Taylor, P., Thomas, J., Sinha, N., Dauwels, J., Kaiser, M., Thesen, T., et al. (2015). Optimal control based seizure abatement using patient derived connectivity. *Frontiers in Neuroscience*, *9*, . http://dx.doi.org/10.3389/fnins.2015.00202.

Taylor, P., Wang, Y., Goodfellow, M., Dauwels, J., Moeller, F., Stephani, U., et al. (2014). A computational study of stimulus driven epileptic seizure abatement. *Plos one*, *9*(12), e114316. http://dx.doi.org/10.1371/journal.pone.0114316.

Tenney, J., Duong, T., King, J., & Ferris, C. (2004). FMRI of brain activation in a genetic rat model of absence seizures. *Epilepsia*, *45*, 576–582. http://dx.doi.org/10.1111/j.0013-9580.2004.39303.x.

van Luijtelaar, G., Hramov, A., Sitnikova, E., & Koronovskii, A. (2011). Spike-wave discharges in WAG/Rij rats are preceded by delta and theta precursor activity in cortex and thalamus. *Clinical Neurophysiology*, *122*(4), 687–695. http://dx.doi.org/10.1016/j.clinph.2010.10.038.

Wendling, F., Bellanger, J., Bartolomei, F., & Chauvel, P. (2000). Relevance of nonlinear lumped parameter models in the analysis of depth-EEG epileptic signals. *Biological Cybernetics*, *83*, 367–378. http://dx.doi.org/10.1007/s004220000160.

Wendling, F., Benquet, P., Bartolomei, F., & Jirsa, V. (2016). Computational models of epileptiform activity. *Journal of Neuroscience Methods*, *260*, 233–251. http://dx.doi.org/10.1016/j.jneumeth.2015.03.027.

Westmijse, I., Ossenblock, P., Gunning, B., & van Luijtelaar, G. (2009). Onset and propagation of spike and slow wave discharges in human absence epilepsy: A MEG study. *Epilepsia*, *50*, 2538–2548. http://dx.doi.org/10.1111/j.1528-1167.2009.02162.x.

Williams, D. (1953). A study of thalamic and cortical rhythms in petit mal. *Brain*, *76*, 50–69. http://dx.doi.org/10.1093/brain/76.1.50.